

See discussions, stats, and author profiles for this publication at: <https://www.researchgate.net/publication/338503303>

Polarization-Diversity Microring-Based Optical Switch Fabric in a Switch-and-Select Architecture

Conference Paper · January 2020

DOI: 10.1364/OFC.2020.Th3B.2

CITATIONS

0

READS

84

4 authors, including:



[Qixiang Cheng](#)

University of Cambridge

83 PUBLICATIONS 719 CITATIONS

[SEE PROFILE](#)



[Rui Chen](#)

Columbia University

1 PUBLICATION 0 CITATIONS

[SEE PROFILE](#)



[Keren Bergman](#)

Columbia University

592 PUBLICATIONS 10,058 CITATIONS

[SEE PROFILE](#)

Some of the authors of this publication are also working on these related projects:



Wide Area Networking [View project](#)



CENTER FOR INTEGRATED ACCESS NETWORKS - CIAN [View project](#)

Polarization-Diversity Microring-Based Optical Switch Fabric in a Switch-and-Select Architecture

Hao Yang, Qixiang Cheng*, Rui Chen, Keren Bergman

Department of Electrical Engineering, Columbia University, New York, NY, 10027, USA

*Author e-mail address: qc2228@columbia.edu

Abstract: We propose a polarization-diversity microring-based optical switch fabric in a switch-and-select architecture with polarization splitter-rotators. The first primitive 2×2 silicon device is demonstrated with polarization-dependent loss of <1.6 dB and inter-channel crosstalk of <-45 dB.

1. Introduction

With the rapid expansion of modern datacenters, the optical interconnect is playing an increasingly important role in delivering high bandwidth communication connectivity among the numerous servers [1]. Optical switches have shown to be a potential key element to meet the growing interconnection requirements in datacenters, based on technologies including micro-electro mechanical systems (MEMSs) [2], liquid crystals on silicon (LCOSs) [3], and micro-ring resonators (MRRs) [4, 5]. Microring-based silicon photonic switches exhibit advantages such as small footprint and high energy efficiency, and demonstrated the potential for high scalability [5]. In addition to the insertion loss and crosstalk, polarization sensitivity is one of the remaining challenge in optical switches for practical employment. However, most of demonstrations were limited to single-polarization so far and current designs that address polarization sensitivity are mainly reported for Mach-Zehnder interferometer (MZI)-based designs [6, 7].

In this paper, we propose and demonstrate a polarization-diversity MRR-based optical switch fabric in the switch-and-select architecture with polarization splitter-rotators (PSRs). This first primitive 2×2 silicon device is designed and demonstrated incorporating 8 thermally actuated MRRs, 4 PSRs and a central shuffle network. Test results reveal the chip polarization-dependent loss to be below 1.6 dB. This switch device further exhibits inter-channel crosstalk of lower than -45 dB and an extinction ratio better than 45 dB due to the switch-and-select topology.

2. Device design, fabrication and packaging

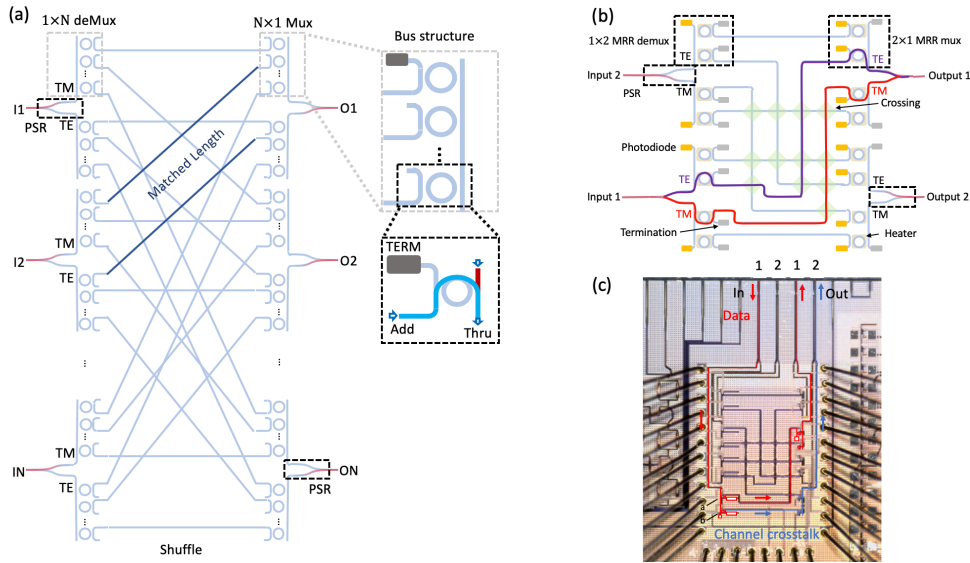


Figure 1. (a) Schematic of $N \times N$ MRR-based polarization diversity switch in switch-and-select architecture. (b) Schematic of the 2×2 Si MRR-based polarization diversity switch fabric. (c) Microscope photo of the fabricated device.

The $N \times N$ polarization diversity in switch-and-select architecture is constructed by PSRs and MRR add-drop filters assembled in a $1 \times N$ bus structure acting as spatial (de)multiplexers, as shown in Fig. 1(a). Scale-up of such a device only requires adding microrings to the bus waveguides, significantly reducing scaling overhead in loss [2]. The increased complexity of central shuffle network as a function of port counts can be leveraged by a two-layered structure [2]. The shuffling length for the TE and TM pair for the same input and output port is designed to be equal

to minimize the differential group delay (DGD). A schematic of the 2×2 polarization insensitive switch-and-select switch, designed with AIM PDKs is shown in Fig. 1 (b). A TE&TM edge coupler is used at a pitch of 127 μm enabling efficient coupling for both TE and TM-polarized light coupling to or from the fiber. A PSR is followed to split the light into its TE and TM polarization eigenstate, and the TM component is subsequently rotated to become TE. The two components then pass a dual 2×2 MRRs based switch-and-select switch, through the port-to-port TE/TM path separately (shown in Fig. 1(b)). The add-drop MRR element is designed to operate close to its critical coupling to maximize the extinction of resonance and minimize the drop loss. The tuning of the microring is accomplished through an integrated micro-heater.

Terminations are placed at the through port of the 2×1 MRR mux and add ports of the 1×2 demux to eliminate optical reflections. Photodiodes (PD) are integrated at the through port of input path to provide on-chip monitoring of the device and polarization state of input light. The central shuffle network is implemented in Si layer with 12 crossing. The device was fabricated through the AIM Photonics MPW run. The 2×2 switch fabric (shown in Fig. 1(c)) has a compact footprint of $0.9 \times 1.5 \text{ mm}^2$, with 16 control electrodes, 12 monitor electrodes, and 4 common grounds. The bare die was wire-bonded onto a breakout PCB as shown in Fig. 2(a) and (b).

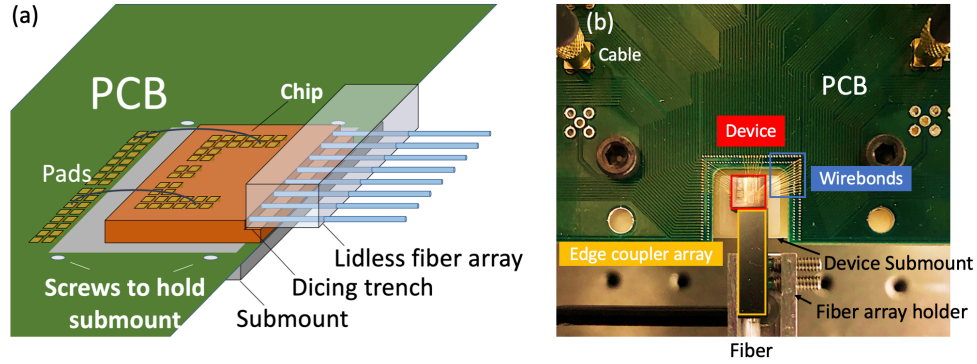


Figure 2. (a) Schematic of a silicon die wire bonded onto a breakout PCB. A lidless fiber array is attached to the edge of the silicon chip. (b) Photo of the packaged AIM switch device by wire bonding on the breakout PCB.

A single-mode lidless fiber array was attached to the chip to couple light into and out of the whole chip, allowing minimum distance within the dicing trench as shown in Fig. 2(a). Two pairs of looped-back edge coupler were introduced to facilitate the coupling process and determine the coupling loss, at $\sim 5.4 \text{ dB/facet}$, as a reference.

3. Device characterization

The experiment test-bed is schematically shown in Fig. 3. A tunable laser is used to launch a continuous-wave signal into the chip. A polarization controller is followed to determine the polarization state of input light. The output is connected to a lightwave multimeter to record the transfer power. A TE/TM eigenstate at a path is achieved by maximizing the power for the corresponding output when only the two MRRs on the path are on resonance (referring back to Fig. 1(b)). The polarization state is also monitored by digital multimeters connected to photodiodes at the through port at each path as a reference. The drop transfer function under the two MRR operation (shown in Fig. 4(a)) is first accessed by tuning the wavelength of input light and monitoring at path 1-1 TM (referring back to red path in Fig. 1(c)). This filtering profile shows a 3-dB bandwidth of 50GHz. The operation wavelength is then selected to be close to the half FSR of MRRs to the resonance, i.e. 1555.0 nm, in the following experiments.

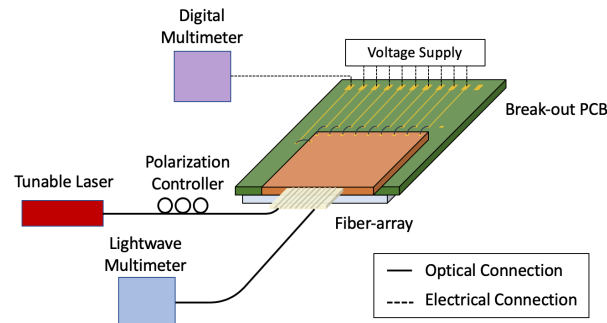


Figure 3. Schematic of the device testbed.

Tuning of the MRR resonance, as shown in Fig. 4(b) is achieved by applying a bias on the n-doped thermal phase shifter embedded in the MRR and monitoring for path 1-1 TM. The off-set voltages of both phase shifters are 1.78V and 1.86V respectively. The profile of a single-stage and a two-stage MRRs on a path shows on-off extinction of >30dB and the path extinction ratio of >45dB. This measured path extinction ratio, which is smaller than square of the MRR on-off extinction, is believed mainly due to the crossing in the shuffle network.

The port-to-port power transfer function is then examined at each path to provide the performance characteristics of the switch device, i.e. insertion loss, polarization crosstalk and channel-to-channel crosstalk. Fig. 4(c) shows the measured optical power map of the switch fabric. Data on 6 optical paths, i.e. input 1TM/1TE – output 1TM/1TE, input 2TM/2TE – output 1TM/1TE, input 2TM/2TE – output 2TM/2TE, are recorded out of the total 8 paths due to 2 electrical open circuits. Optical paths exhibit on-chip losses in the range of -4 dB to -7.8 dB are presented in Fig. 4(c) outlining in a red box. The distinction of polarization dependent insertion loss is as low as 1.6dB for each path. The low polarization dependent loss is attributed to the reverse placement of the polarization splitter rotator at the output (shown in Fig. 1(b)). As a result, the light encounters the same insertion loss of both TE to TM and TE to TE from PSR once for each polarization component.

To measure the inter-channel crosstalk, as illustrated in Fig. 1(c), the data is routed through path 1-1TM, and the inter-channel crosstalk is monitored at 2TM. In the outlined input 1×2 spatial deMux unit, the MRR at path 1-1TM (element a) is at an off-resonance state to bypass the signal. The MRR at path 1-2 TM (element b), which receives the channel-to-channel crosstalk leakage, is set at on-resonance state. The measured inter-channel crosstalk is shown in Fig. 4(c) outlining in a blue box as low as <-45dB. Both the degradation of extinction ratio and channel-to-channel crosstalk from expected is believed to be originated from the crosstalk of Si crossing in the shuffle network. This, however, can be significantly improved by optimizing the component design and fabrication in the future.

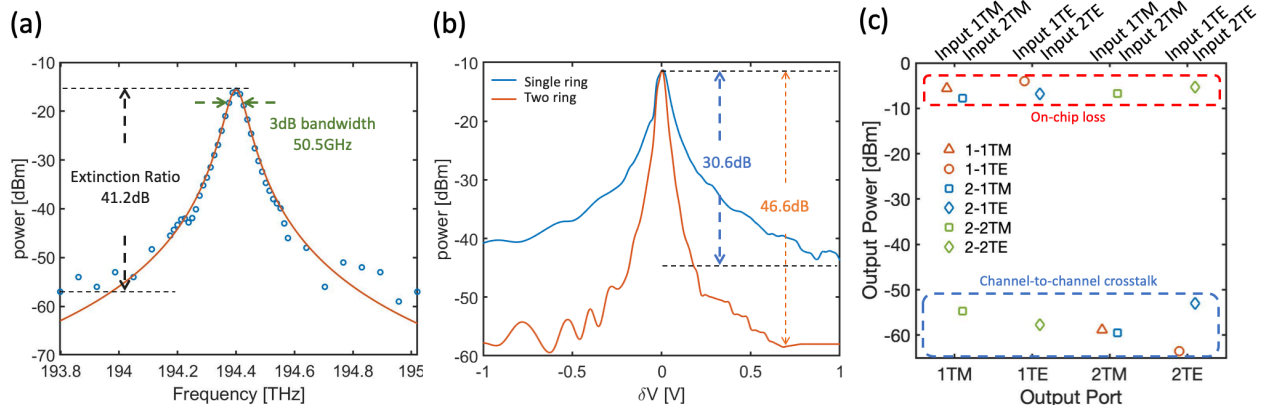


Figure 4. (a) Dual-ring spectrum at path 1-1TM. (b) Power transfer vs. bias-voltage on the MRR at path 1-1TM. (c) Measured optical power map of the 2×2 MRR-based polarization insensitive switch-and-select device.

4. Conclusion

The first polarization diversity microring-based optical router in switch-and-select topology is presented. The thermally actuated 2×2 port device is fully packaged via wire-bonding. Power transfer function reveals the on-chip loss is down to -4 dB, with both crosstalk suppression and extinction ratio as high as over 45dB. The polarization dependent loss is within 1.6 dB. This device shows superior performance for both polarization states of input light and great potential for high-performance switching applications in datacenters.

References

- [1] Q. Cheng et al, "Photonic switching in high performance datacenters [Invited]," *Opt. Express*, **26**, 16022-16043 (2018)
- [2] K. Tanizawa et al, "Non-duplicate polarization-diversity 8×8 Si-wire PILOSS switch integrated with polarization splitter-rotators," *Opt. Express*, **25**, 10885-10892 (2017)
- [3] B. Robertson et al, "Demonstration of multi-casting in a 1×9 LCOS wavelength selective switch," *J. Light. Technol.*, **32**, 402-410 (2013)
- [4] Q. Cheng et al, "Ultralow-crosstalk, strictly non-blocking microring-based optical switch," *Photonics Res.*, **7**, 155-161 (2019)
- [5] Q. Cheng et al, "Scalable microring-based silicon cros switch fabric with switch-and-select stages," *IEEE J. Sel. Top. Quantum Electron.*, **25**, 1-11 (2019)
- [6] K. Tanizawa et al, "Non-duplicate polarization-diversity 8×8 Si-wire PILOSS switch integrated with polarization splitter-rotators." *Opt. Express*, **25**, 10885-10892 (2017)
- [7] S. Wang & D. Dai, "Polarization-insensitive 2×2 thermo-optic Mach-Zehnder switch on silicon." *Opt. Lett.*, **43**, 2531-2534 (2018)